

Photosynthetic physiologies of phytoplankton in the eastern equatorial Indian Ocean during the spring inter-monsoon

Chao Yuan^{1, 2}, Zongjun Xu², Xuelei Zhang^{2*}, Qinsheng Wei², Huiwu Wang³, Zongling Wang^{1, 2}

¹ College of Environment Science and Engineering, Ocean University of China, Qingdao 266061, China

² Marine Ecology Research Center, MNR Key Laboratory of Science and Engineering for Marine Ecosystems, First Institute of Oceanography, Ministry of Natural Resources, Qingdao 266061, China

³ MNR Key Laboratory of Marine Science and Numerical Modeling, First Institute of Oceanography, Ministry of Natural Resources, Qingdao 266061, China

Received 12 January 2018; accepted 22 March 2018

© Chinese Society for Oceanography and Springer-Verlag GmbH Germany, part of Springer Nature 2019

Abstract

Phytoplankton physiologies are dynamic and have sensitive responses to the ambient environment. In this paper, we examine photosynthetic physiologies of phytoplankton communities with Phyto-PAM in the eastern equatorial Indian Ocean during the spring inter-monsoon. Environmental parameters were measured to investigate the coupling between phytoplankton photosynthetic physiologies and their habitats. During the cruise, the water column was highly stratified. The mixed layer extended to about 75 m and was characterized by high temperature (>28°C) and low nutrient level. The F_v/F_m values and chlorophyll *a* (Chl *a*) concentrations were lower at the surface, as consequences of nutrient depletion and photo-inhibition. Subsurface Chl *a* maximum (SCM) occurred between 75 and 100 m, and had the highest F_v/F_m values. The formation of SCM was a balance between nutrient availability and light limitation. The SCM may contribute significantly to pelagic food web and primary production in the water column. Phytoplankton in different layers encountered different light, trophic and hydrographic dynamics and evolved distinct photosynthetic characteristics. Despite of co-limitation of nutrient limitation and photo-inhibition, phytoplankton in the surface layer showed their acclimation to high irradiance, had lower light utilization efficiencies (α : 0.061 ± 0.032) and could exploit a wide range of light irradiance. Whereas, phytoplankton in the SCM layers presented the highest light utilization efficiencies (α : 0.146 ± 0.48), which guaranteed higher photosynthetic capacities under low light level. These results provide insights into phytoplankton photo-adaptation strategies in this less explored region.

Key words: F_v/F_m , rapid light curves, photosynthetic physiologies, eastern equatorial Indian Ocean

Citation: Yuan Chao, Xu Zongjun, Zhang Xuelei, Wei Qinsheng, Wang Huiwu, Wang Zongling. 2019. Photosynthetic physiologies of phytoplankton in the eastern equatorial Indian Ocean during the spring inter-monsoon. Acta Oceanologica Sinica, 38(6): 83–91, doi: 10.1007/s13131-018-1218-0

1 Introduction

Phytoplankton are the main primary producers in the marine ecosystems, and account for nearly half of global net primary production (Field et al., 1998). Their photosynthetic organic matters sustain the pelagic food web and provide carbon source for marine biogeochemical cycle. The photosynthetic physiologies of phytoplankton are dynamic and highly responsive to the environment (Halsey and Jones, 2015). Chlorophyll *a* (Chl *a*) fluorescence provides a rapid, sensitive and non-intrusive method to assess photosynthetic physiologies of phytoplankton communities (Schreiber, 2004; Suggett et al., 2010).

F_v/F_m , the maximum quantum yield of photosystem II after dark adaptation, is often used as an indicator of photo-physiological state (Kalaji et al., 2012; Schreiber et al., 1995). For instances, in coastal eutrophic waters, phytoplankton exhibit higher F_v/F_m . Diatoms dominated in the Daya Bay and their F_v/F_m could reach up to 0.72 (Wang et al., 2012). Li and Sun (2014) reported phytoplankton maintained higher F_v/F_m value in winter, which would

lead to phytoplankton bloom in spring in the Jiaozhou Bay. In high nutrient, low Chl *a* waters, photosynthetic activities were depressed by iron limitation, addition of Fe stimulated accumulation of phytoplankton biomass and enhanced photosynthetic capacity (F_v/F_m) significantly (Moore et al., 2007; Hopkinson et al., 2007). In the Taihu Lake, F_v/F_m presented significant diurnal variation and photo-inhibition affected the instantaneous growth rates of phytoplankton (Zhang et al., 2008). F_v/F_m has been an effective indicator of environment stresses, such as nutrient limitation, photo-inhibition and toxicities (Barlow et al., 2017; Kim Tiam et al., 2015; White et al., 2011).

Rapid light curves (RLCs) is determined by consecutive measurements of functional quantum yield after short time exposures to progressively increasing irradiance (Schreiber, 2004). Three cardinal photosynthetic parameters can be obtained from RLCs, which are α (initial slope of the curve; represents light utilization efficiencies), $rETR_{max}$ (maximum relative electron transport rate under saturating irradiance) and I_k (minimal saturation light irra-

Foundation item: The Global Change and Air-Sea Interaction Program under contract No. GASI-03-01-03-03; the S&T Innovation Project of the Qingdao National Laboratory for Marine Science and Technology under contract No. 2016ASKJ14; the FIO Basic Research Fund under contract No. 2013T04.

*Corresponding author, E-mail: zhangxl@fio.org.cn

diance) (Schreiber, 2004; Harrison et al., 2015). RLCs can assess not only the present photosynthetic capacities, but the potential photosynthetic activity over a wide range of light intensities (Ralph and Gademann, 2005). The photosynthetic characteristics of phytoplankton differ markedly due to differences in nutrient uptake, photo-adaptation and environment sensing (Halsey et al., 2014). In high eutrophic coastal waters, phytoplankton acclimated to relative brighter light dominated the upper stratified waters, while autotrophies acclimated to lower light dominated the mixed waters (Mino et al., 2014). Diatoms had rapidly inducible non-photochemical quenching (NPQ), and maintained high photochemical activities over a wide range of light intensity in coastal area (Lavaud et al., 2007; Li and Sun, 2014; Wang et al., 2012). In contrast, low light adapted eco-types, such as benthic alga and bottom ice alga (Hartig et al., 1998), reached the light saturating point at lower light intensity, and suffered from photo-inhibition under higher light (McMinn and Hegseth, 2004).

The Wyrтки jets occur regularly during boreal spring inter-monsoon in the eastern equatorial Indian Ocean (EEIO) (Wyrтки, 1973; Schott and McCreary, 2001). The main consequence of Wyrтки jets is the depression of thermocline and nitracline in the EEIO (Wiggert et al., 2006). Therefore, EEIO has low primary productivities during the inter-monsoon period, which can be manifested by satellite observation of surface Chl *a* concentrations (Fig. 1). Previous shipboard investigations have substantiated this observation. Xue et al. (2016) reported the diatoms communities were dominated by tropical and warm oceanic species, in line with their environmental characteristics. Hong et al. (2012) reported that EEIO was highly stratified with surface Chl *a* concentration lower than 0.10 mg/m³, and pico-phytoplankton dominated the contribution to total Chl *a* biomass. Moreover, persistent subsurface chlorophyll *a* maximum (SCM) was developed and contributed significantly to Chl *a* biomass and primary production in the water column (Li et al., 2012; Liu et al., 2011). However, it remains unclear about the photosynthetic characteristics of phytoplankton in the EEIO.

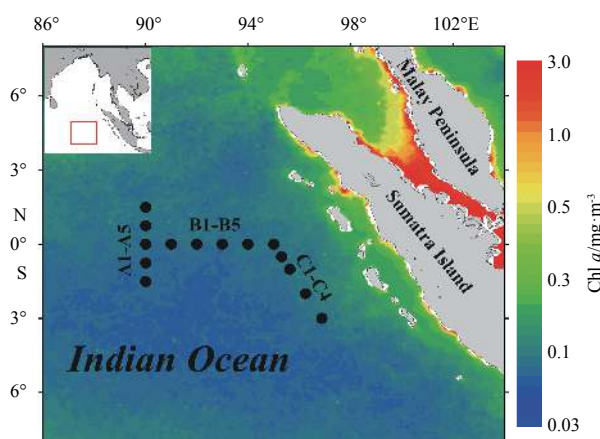


Fig. 1. Sampling stations overlaid on the climatological May monthly SeaWiFS Chl *a* in the eastern equatorial Indian Ocean. Data were obtained from NOAA Ocean Watch website: <http://oceanwatch.pifsc.noaa.gov/>.

In highly stratified waters of the EEIO, phytoplankton in different layers encounter distinct different light, hydrographic and trophic dynamics. Therefore, we hypothesized that these autotrophic organisms could have different photosynthetic characteristics and evolve different adaptation strategies. In this study, we

used Phyto-PAM to assess photosynthetic physiologies of phytoplankton communities in the eastern equatorial Indian Ocean during the boreal spring inter-monsoon. Environmental factors such as temperature, salinity and macro-nutrients were also measured. Our study aimed to understand the different photosynthetic characteristics of phytoplankton in the context of stratification. We also attempted to explain their correlations with environmental factors and the potential influence on pelagic carbon cycles.

2 Materials and methods

2.1 Hydrography and chemistry

The study included 15 stations in three transects in the EEIO (Fig. 1) and was conducted onboard the R/V *Madidihang 03* from April 26 to May 14 of 2012. Transect A comprised five stations (2°S–2°N along 90°E). Transect B included five stations along the equator from 91°E to 95°E. Transect C was paralleled to the Sumatra Island with four stations from 0°, 95°E to 4°S, 97.5°E.

At each station, CTD casts were conducted to obtain the vertical profiles of temperature and salinity. The depth of 28°C isotherm was defined as the mixed layer depth. Seawater samples were collected from eight discrete depths (3, 25, 50, 75, 100, 125, 150 and 200 m) by the attached 5 L Niskin bottles for chemical and biological analyses. Samples for dissolve inorganic nitrogen (nitrite and nitrate, DIN), and phosphate (DIP) determinations were collected in polypropylene bottles and analyzed with a SKALAR SANplus nutrient analyzer. The depth of 2 μmol/L nitrate isoline was considered as the base of nitracline. The euphotic depth (depth of 1% surface light intensity) was estimated by 2.7 times of the transparency depth measured with Secchi disc at day time (Idso and Gilbert, 1974).

2.2 Biology

2.2.1 Chl *a*

A total of 113 seawater samples were collected for the estimation of Chl *a* concentrations. For each sample, an aliquot of 1 L seawater was filtered on Waterman GF/F filters, which was then stored at –20°C in dark until analysis. The filters were extracted in 90% acetone overnight at 0°C, and Chl *a* concentrations were measured by calibrated Turner Design 10-AU fluorometer (Parsons et al., 1984).

2.2.2 PAM fluorometry

Phytoplankton's photosynthetic physiologies were measured by Phyto-PAM (Waltz, Germany). All measured data were corrected by subtracting the background fluorescence of filtered seawater (GF/F, Waterman). After 20 min of dark adaption, minimum fluorescence (F_0) was determined by a weak modulated measuring light, and then a 200 ms saturating pulse was applied to determine maximum fluorescence (F_m). F_v/F_m was calculated as $(F_m - F_0)/F_m$.

In RLCs measurement, the actinic irradiances (1, 16, 32, 64, 164, 264, 364, 464, 564, 664 and 764 μmol/(m²·s)) were applied for 10 s (Schreiber, 2004; Ihnken et al., 2010). Each irradiance was followed by 200 ms saturating pulse to determine functional quantum yield (Φ_{PSII}). The relative electron transport rates ($rETR = 0.42 \times E \times \Phi_{PSII}$) were calculated by multiplying the actinic irradiance with functional quantum yield (Schreiber, 2004). RLCs were fitted with the model proposed by Eilers and Peeters (1988), and the photosynthetic parameters (α , $rETR_{max}$ and E_k) were estimated with Phytowin v2.1.3 software (Waltz, Germany).

2.3 Statistical analysis

The vertical profiles of environment factors were plotted with Sigmaplot 12.5. All statistics were analyzed with SPSS 17.0. Two-way ANOVA was used to determine the overall differences of temperature, salinity, nutrient and biological variables among different station and depth. The Student's Least Significant Difference test (LSD) was used to compare the differences between depths. Contour maps in Ocean Data View were used to explore the variations of Chl *a* concentrations and F_v/F_m in the water column. A subset of data ($N=70$) that included data above the euphotic zone (>100 m) were used to explore the relationships between photosynthetic characteristics and environmental factors by Pearson's correlation.

3 Results

3.1 Hydrography and chemistry

The water column was stratified during the cruise (Figs 2, 3 and Table 1). The mixed layer extended to about 75 m. In the

mixed layer, temperature was more than 29.38°C, whereas salinity ranged from 34.15 to 34.40 (Table 1). The thermocline presented at the depth between 75 m and 100 m (Fig. 2). Temperature decreased from $(29.38\pm 0.51)^\circ\text{C}$ to $(20.58\pm 1.07)^\circ\text{C}$, while salinity increased from 34.40 ± 0.13 to 35.30 ± 0.09 (Fig. 3). Below the thermocline, salinity remained above 35.0, while temperature decreased continuously and reached $(14.74\pm 0.46)^\circ\text{C}$ at 200 m (Fig. 3). The euphotic depth ranged from 81 m to 116 m, with mean value of 99 m. The maximum euphotic depth was found at B4 (Fig. 2).

In the mixed layer, nutrients were depleted, with mean nitrate and DIP concentrations less than $2.82\ \mu\text{mol/L}$ and $0.45\ \mu\text{mol/L}$, respectively (Fig. 3 and Table 1). In concomitance with thermocline, mean nitrate and DIP concentrations tripled (Fig. 3), with values of $(9.08\pm 4.10)\ \mu\text{mol/L}$ and $(1.15\pm 0.48)\ \mu\text{mol/L}$ at 100 m, respectively (Table 1). Moreover, primary nitrite maximum (PNM) was formed within the thermocline (Table 1). Below 125 m, DIN and DIP concentrations continued to increase with depth, reached $(15.60\pm 8.44)\ \mu\text{mol/L}$ and $(2.10\pm 0.55)\ \mu\text{mol/L}$ at 200 m, respectively (Fig. 3 and Table 1). The DIN/DIP molar ratios were

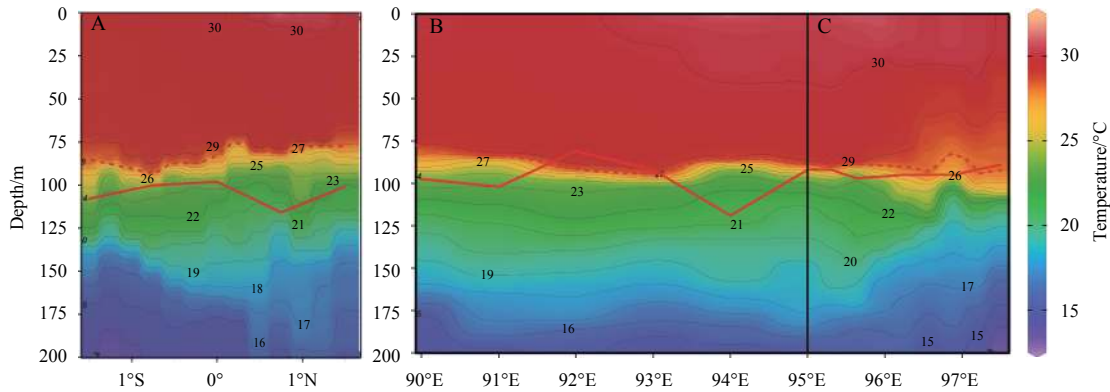


Fig. 2. Vertical distribution of temperature along Transects A, B and C in the eastern equatorial Indian Ocean. Red dotted line represented 28°C, as a proxy of the mixed layer depth. Red solid line indicated the euphotic depth.

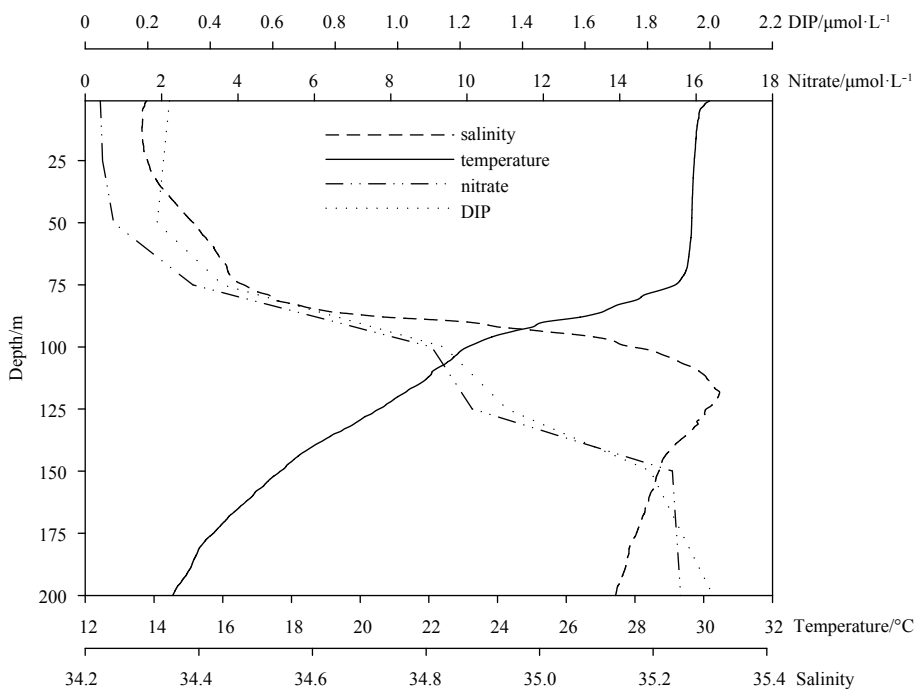


Fig. 3. Vertical profiles of average temperature, salinity, nitrate and DIP for the 14 stations in the eastern equatorial Indian Ocean.

Table 1. Summary statistics of environmental factors (mean±standard deviation) for the 14 stations in the EEIO

Depth/m	Temperature/°C	Salinity	Nitrite/ $\mu\text{mol}\cdot\text{L}^{-1}$	Nitrate/ $\mu\text{mol}\cdot\text{L}^{-1}$	DIP/ $\mu\text{mol}\cdot\text{L}^{-1}$	DIN/DIP ratio
3	30.19±0.36 ^a	34.15±0.19 ^a	0.026±0.016 ^a	0.39±0.27 ^a	0.27±0.09 ^a	1.73±1.27 ^a
20	29.98±0.26 ^{ab}	34.22±0.11 ^a	0.032±0.020 ^a	0.45±0.35 ^a	0.25±0.11 ^a	2.08±1.50 ^a
50	29.68±0.23 ^{ab}	34.33±0.10 ^b	0.028±0.013 ^a	0.74±0.82 ^a	0.23±0.06 ^a	3.48±3.53 ^{ab}
75	29.38±0.51 ^b	34.40±0.13 ^b	0.086±0.074 ^b	2.82±2.33 ^a	0.44±0.18 ^a	5.95±4.47 ^{ab}
100	23.31±1.07 ^c	35.08±0.19 ^c	0.181±0.095 ^c	9.08±4.10 ^b	1.15±0.48 ^b	8.20±3.47 ^{bc}
125	20.58±1.07 ^d	35.30±0.09 ^d	0.057±0.041 ^a	10.14±3.15 ^b	1.35±0.53 ^b	8.09±2.74 ^c
150	18.41±1.02 ^e	35.23±0.04 ^d	0.040±0.014 ^a	15.38±5.78 ^c	1.81±0.57 ^c	8.80±2.78 ^c
200	14.74±0.46 ^f	35.13±0.01 ^c	0.049±0.020 ^a	15.60±8.44 ^c	2.10±0.55 ^c	8.30±5.47 ^c

Note: The superscript letters a–f next to the digits indicated statistical difference between the means at depths ($p < 0.05$, LSD).

largely deviated from Redfield ratio of 16:1. The mean DIN/DIP ratio was 1.73 ± 1.27 at the surface, and increased with depth. It reached 8.20 ± 3.47 at 100 m and was relatively stable below.

3.2 Chl *a* and photosynthetic characteristics

The surface Chl *a* concentrations were lower than 0.10 mg/m^3 , similar to remote sensing data (Fig. 1). The subsurface Chl *a* maximum (SCM) was the persistent feature along the three transects (Fig. 4). The Chl *a* concentrations reached $(0.22 \pm 0.05) \text{ mg/m}^3$ in the SCM, with the maximum (0.35 mg/m^3) at 75 m at C2. The SCM depth maintained 75 m at most stations and was deeper (100 m) at A3 and A4. Below the SCM, Chl *a* concentrations dropped to levels close to or lower than those at surface. The depths of SCM were in concomitance with the mixed layer depth

and euphotic depth (Fig. 4).

Along the three transects, the surface F_v/F_m value varied between 0.09 and 0.42 with mean of 0.27 ± 0.11 (Figs 5 and 6a). The lowest surface F_v/F_m values were recorded in Transect A. Vertically, F_v/F_m values tended to become greater with depth, and reached the maximum in the SCM between 75 m (0.50 ± 0.15) and 100 m (0.52 ± 0.11). For instance, at C2, SCM was found at 75 m, and F_v/F_m value reached 0.70 (Fig. 5).

Figure 6 showed the vertical distribution of main photosynthetic parameters derived from RLCs. F_v/F_m and α presented unimodal changes across the water column and reached the peak at 75 m/100 m. $r\text{ETR}_{\text{max}}$ were not significantly different in the upper 100 m water column, and were lower at deeper layers. I_k in general decreased from surface to deeper layers. The mean values of α

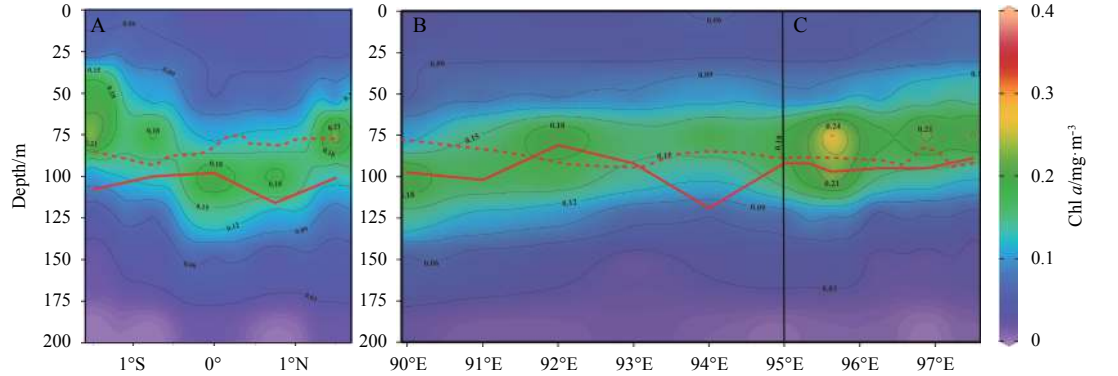


Fig. 4. Vertical distribution of Chl *a* along Transects A, B and C in the eastern equatorial Indian Ocean. Red dotted line represented 28°C, as a proxy of the mixed layer depth. Red solid line indicated the euphotic depth.

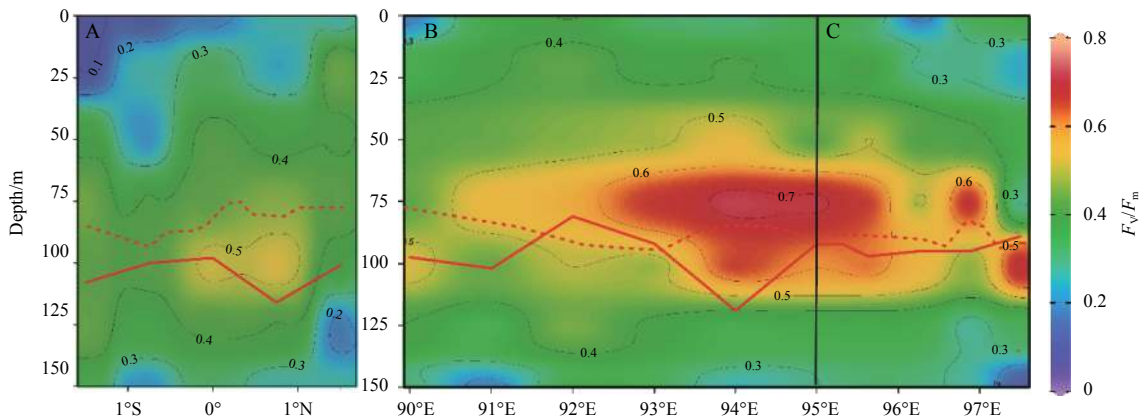


Fig. 5. Vertical distribution of F_v/F_m along Transects A, B and C in the eastern equatorial Indian Ocean. Red dotted line represented 28°C, as a proxy of the mixed layer depth. Red solid line indicated the euphotic depth.

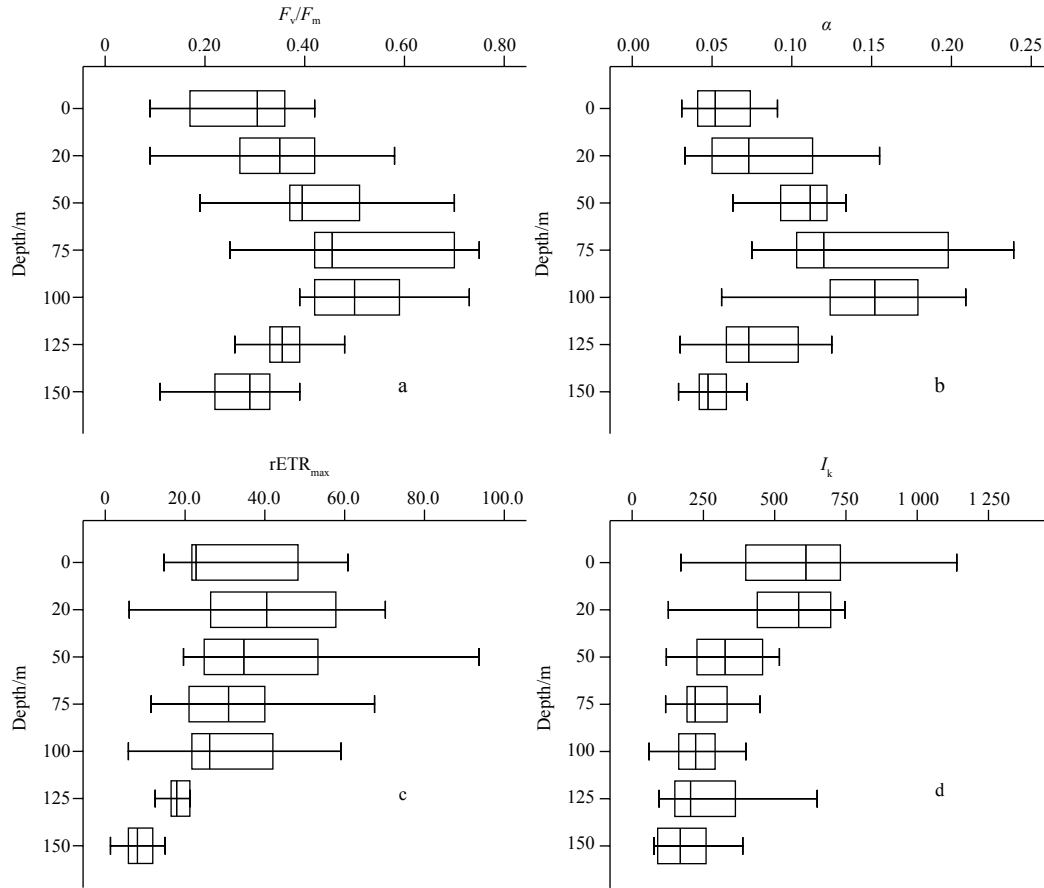


Fig. 6. Variation of photosynthetic parameters (F_v/F_m , α , $rETR_{max}$, I_k) in the eastern equatorial Indian Ocean. For each parameters, the letters next to bars indicated statistical differences ($p < 0.05$) between the means at depths. For each box, the left and right were the first and third quartiles; the band inside the boxes was the median; the ends of whiskers represented the minimum and maximum except outliers.

ranged 0.06–0.15, with peak values occurring at 100 m (Fig. 6b). The mean values of $rETR_{max}$ varied 9–55, with the maximum at 20 m (Fig. 6c). I_k varied from $(615 \pm 296) \mu\text{mol}/(\text{m}^2 \cdot \text{s})$ at surface to $(185 \pm 95) \mu\text{mol}/(\text{m}^2 \cdot \text{s})$ at 150 m (Fig. 6d).

3.3 Pearson’s correlations between environmental and photosynthetic parameters

Encountered with different environmental factors, phytoplankton revealed different photochemical responses. Pearson’s correlations were performed to determine the relationships between photosynthetic parameters and environment factors in the euphotic zone (≤ 100 m) (Table 2). Chl *a* was significantly positively correlated with depth, salinity, nitrite and nitrate. F_v/F_m and α showed similar relationships, in addition to significantly positive correlations with nitrate and DIN. On the contrary, E_k is significantly negatively correlated with depth, nitrite, DIP

and salinity, while positively related with temperature. The results also suggested that $rETR_{max}$ had no significant relationships with measured environmental factors.

Correlations among photosynthetic parameters were also significant. Chl *a*, F_v/F_m and α , were positively correlated with each other, while showed negative relationship with E_k . This indicated that low light acclimated phytoplankton had higher photosynthetic competence and light utilization efficiencies than high light acclimated counterparts in the EEIO.

4 Discussion

4.1 Limitations by nutrient depletion and photo-inhibition at sea surface

The significant vertical variations of Chl *a* and F_v/F_m suggested stratification remarkably influenced the biomass and

Table 2. Pearson’s correlations between environmental and photosynthetic parameters in the euphotic zone of EEIO

	Depth	Temperature	Salinity	Nitrite	Nitrate	DIN	DIP	Chl <i>a</i>	F_v/F_m	α	$rETR_{max}$
Chl <i>a</i>	0.62**	-0.17	0.27*	0.26*	0.29*	0.32**	0.19		0.47**	0.48**	-0.24*
F_v/F_m	0.60**	-0.37**	0.42**	0.29*	0.43**	0.48**	0.41**	0.47**		0.77**	0.27*
<i>A</i>	0.62**	-0.43**	0.49**	0.24	0.48**	0.56**	0.46**	0.48**	0.77**		0.34**
$rETR_{max}$	-0.13	0.16	-0.13	-0.17	-0.16	-0.08	-0.18	-0.05	0.27*	0.34**	
E_k	-0.54**	0.40**	-0.40**	-0.36**	-0.41**	-0.40**	-0.43**	-0.39**	-0.24*	-0.37**	0.65**

Note: * Correlation is significant at the 0.05 level (two-tailed); ** correlation is significant at the 0.01 level (two-tailed).

physiologies of photosynthetic organisms. In consistence with many studies in highly stratified waters (Hong et al., 2012; Li et al., 2012; Thompson et al., 2007), we observed low surface chlorophyll *a* concentrations and photosynthetic competence. The scarcity of nutrients limited the growth of phytoplankton, with mean nitrate concentrations less than 2 $\mu\text{mol/L}$ in the upper mixed layer (Table 1). In addition, large deviation of Redfield ratio was found with mean DIN:DIP ratio less than 5 (Table 1 and Fig. 3), similar to former study at 83°E in the equatorial Indian Ocean (Sardessai et al., 2010). Therefore, phytoplankton in the surface layer were nitrogen limited. Moreover, there was little nutrient enrichment from deep water due to weak surface winds and thermocline depression caused by Wyrтки jet (Wyrтки, 1973). As nitrogen concentrations in the mixed layer were very low, there was no capacity for a significant increase in phytoplankton biomass without additional nitrogen inputs (Thompson et al., 2007). In contrast, the observed surface Chl *a* increase was always associated with vertical mixing and nutrients enrichment. For instances, bi-weekly Chl *a* spikes were reported at central equatorial Indian Ocean during fall, and Strutton et al. (2014) attributed to the advection of water and nutrient entrainment by local mixing. Similarly, higher surface Chl *a* concentrations were found in the subtropical convergence zone of south-western Indian Ocean, where obvious increase of nitrate and DIP concentrations at sea surface occurred (Hong et al., 2012).

Nutrients limitations would impair normal cellular processes such as photosynthesis and some enzyme activities. Halsey and Jones (2015) reported that decreased allocation of carbon to cellular proteins was a fundamental adaptive nitrate stress response among many algal taxa. Similarly, phosphorus limitation caused decrease of ATP synthesis and ultimately led to a decline of F_v/F_m (Lippemeier et al., 2001). The growth of phytoplankton in the surface layer could also be limited by excessive light exposure. The photosynthetic active radiation could reach more than 1 800 $\mu\text{mol}/(\text{s}\cdot\text{m}^2)$ at noon (data were acquired from another cruise in May, 2013), which might induce photo-inhibition and damage the activity of photosynthesis (Bouchard et al., 2005). Even at the surface of well-mixed environment, the increase of photo-protection pigment and decrease of F_v/F_m occurred, indicating some photo-protection and photo-inhibition under high light (Barlow et al., 2017). Therefore, co-limitation of nutrient de-

pletion and photo-inhibition resulted in lower photosynthetic competence (F_v/F_m) and Chl *a* biomass in the upper mixed layer, especially in Transect A.

4.2 Prevalence of SCM and its importance in pelagic primary production

The SCM tends to be permanent feature in stratified tropical oceans and occur seasonally in temperate and Arctic waters (Cullen, 2015; Martin et al., 2010). Combined with formal studies, we found that the SCM was common across the tropical Indian Ocean (Table 3). The SCM depth during our cruise was similar with previous studies in the EEIO, south equatorial current of Indian Ocean as well as Bay of Bengal (Li et al., 2012; Zhou et al., 2011; Liu et al., 2011), shallower than Indian Ocean subtropical gyre (Thompson et al., 2007; George et al., 2013), while deeper than some stations where nitracline/thermocline rise occurred (Hong et al., 2012). Though the depth of SCM varied, the depth of SCM was in association with nitracline, indicating the control of nitrate on phytoplankton growth. Lee et al. (2017) reported that the nutrients supply from the lower layers contributed significantly to the maintenance of SCM.

In comparison, the Chl *a* concentrations in the SCM were lower than that of other regions in the Indian Ocean (Table 3). As discussed above, this might be a consequence of weak vertical mixing. Downwelling Kelvin waves propagate eastward along the equator of Indian Ocean (Rao et al., 2010). The strong thermocline right below the SCM layer inhibited water exchange from deep nutrient-riched water. George et al. (2013) reported similar lower Chl *a* concentrations in the western equatorial Indian Ocean during the boreal summer monsoon, and attributed as both the deepening of thermocline and the presence of low-salinity surface waters. In addition, our results indicated the influence of light, as SCM usually occurred at base of euphotic zone (Fig. 4). Therefore, SCM formation was a balance between nutrient availability and light limitation. Other factors, such as photo-acclimation and predator, may also play important roles (Cullen, 2015).

The significant increase of F_v/F_m in the SCM layer suggested that phytoplankton were more photosynthetic competent than the other layers. This was likely because of nutrient depletion through thermocline (Table 1 and Fig. 2), as reported by Li et al.

Table 3. Summary of Chl *a* concentrations (mg/m^3) at the surface and SCM (Chl a_{max}), SCM depth at different regions of Indian Ocean (IO)

Region		Surface	Chl a_{max}	SCM depth/m	Reference
EEIO		0.05	0.22	50–75	this study
South-eastern IO	warm core	0.30	0.40	100	Thompson et al. (2007)
South-eastern IO	cold core	0.09	0.41	90–110	Thompson et al. (2007)
South-western IO	IOSG	0.07	0.59	≥ 100	Hong et al. (2012)
South-western IO	SCZ	0.16–0.26	0.34–0.46	50–70	Hong et al. (2012)
SEC	EIO	0.138	0.30–0.42	60–80	Zhou et al. (2011)
SEC	CIO	0.072	0.26–0.31	75–80	Zhou et al. (2011)
Bay of Bengal	10°S	0.05–0.07		75	Liu et al. (2011)
Central Bay of Bengal	7°–16°N, 88°E	0.06–0.12	>0.25	60–80	Madhupratap et al. (2003)
Western tropical IO	8°N–10°S, 65°E	0.04–0.3	0.30–0.50	50–75	George et al. (2013)
Western tropical IO	10°–18°S, 65°E		0.15–0.30	120	George et al. (2013)
Gascoyne region (WA)	21.3°–26.5°S, 119°–123°E	<0.01	0.4–1.0	60–100	Hanson et al. (2005)

Note: IOSG is Indian Ocean subtropical gyre, SCZ subtropical convergence zone, SEC south equatorial current, EIO eastern Indian Ocean, CIO central Indian Ocean, and WA western Australia.

(2016) and McMinn and Hegseth (2004). F_v/F_m was significantly positively correlated with nitrite, which was an intermediate product of nitrate metabolism mainly released from phytoplankton (Zhang et al., 2016). In concomitance with nitrate metabolism, photosynthesis might be enhanced as well (Li et al., 2016). F_v/F_m was also positively related with Chl *a*. The observed maximum of Chl *a* concentration at 75 m at C2 might be caused by the enhanced photosynthetic activities.

The SCM could contribute significantly to phytoplankton biomass and primary productivities in the water column. For instances, missing real SCM would cause 9.3% underestimation of depth integrated Chl *a* biomass (Li et al., 2012), and the SCM contributed more than half of water column primary production (Liu et al., 2011; Fernand et al., 2013). Though the F_v/F_m values were less in the SCM than that of the coastal waters, such as the Jiaozhou Bay (Li and Sun, 2014) and the Daya Bay (Wang et al., 2012), the SCM was important carbon resource for food web and had important impacts on pelagic carbon cycle (Martin et al., 2010).

4.3 Comparison of photosynthetic characteristics between sea surface and SCM

Photosynthetic characteristics of phytoplankton could be rapidly assessed by RLCs and varied according to *in situ* light history (Ralph and Gademann, 2005; Harrison et al., 2015). We found that the phytoplankton communities had higher E_k and $rETR_{max}$ values in the upper mixed layer than those in the SCM. These results were in consistence with many studies which compared RLCs of photosynthetic organisms under contrasting light and hydrological features. For instances, seagrass *Halophila* growing in shallow waters had substantially higher $rETR_{max}$, E_k than at depth (Durako, 2012; Sharon and Beer, 2008). Ryan et al. (2009) reported surface brine algae had higher $rETR_{max}$ than bottom-ice algae. Under different hydrological structure in coastal eutrophic gulf, cells acclimated to brighter light dominated the upper stratified waters, while cells acclimated to lower light dominated the mixed waters (Mino et al., 2014).

In the upper mixed layer, phytoplankton underwent more dynamic light irradiance, and were challenged to optimize resource allocation to growth and dissipation of excessive light (Wagner et al., 2006). Higher light acclimated autotrophic organisms exhibited higher light saturating points than lower light acclimated counterparts (Ralph and Gademann, 2005). Different trophic status resulted in different responses to high light between diatoms in coastal eutrophic waters and phytoplankton in this oligotrophic region. Diatoms in the coastal eutrophic region had rapidly inducible NPQ and maintained high photochemical activities over a wide range of intensities (Lavaud, 2007; Li and Sun, 2014; Wang et al., 2012), while extremely lower initial slope reflected relatively low photosynthetic activity and productivities at the surface of oligotrophic region (McMinn and Hegseth, 2004).

Photosynthesis states of phytoplankton were gradually shifted from nutrient limitation to light limitation with increasing depth (Table 1). In the SCM, light intensities were 1%–10% of the surface, while nutrients availability increased (Table 1 and Fig. 3). In order to survive, phytoplankton had to be highly adapted to environmental conditions within the thermocline (Sharpley et al., 2001). Phytoplankton in this layer had to increase their efficiency of capturing light, which can be achieved by increasing antenna size and/or the number of antenna. Bibby et al. (2003) indicated that low-light ecotypes of *Prochlorococcus* had much larger antenna than surface ecotypes. The phenotypic response to de-

creased irradiance was dominated by increases in the ratio of PSII reaction centers to carbon fixation capacity within the SCM (Moore et al., 2006). In this study, the higher α guaranteed higher photosynthetic efficiencies under low light circumstances, whereas the lower I_k values suggested low light acclimation in the SCM. Similar to benthic diatoms, ice algae (McMinn and Hegseth, 2004) and *Osterococcus* sp. RCC809 (Six et al., 2008) isolated from the bottom of euphotic zone, phytoplankton in the SCM were adapted to lower light conditions and reached their $rETR_{max}$ at rather lower light. Edwards et al. (2015) reported that open-ocean isolates tended to have higher initial slope than coastal isolates, implying their adaptation to low light. In short, phytoplankton communities in different layers were confronted with variable environment factors, such as light and nutrients, and evolved distinct photosynthetic characteristics.

5 Conclusions

Our results resolve that the eastern equatorial Indian Ocean was an oligotrophic and highly stratified region in the spring inter-monsoon. Here, photosynthetic characteristics in different layers were affected by light and nutrient availability. The low Chl *a* concentrations (<0.10 mg/m³) and F_v/F_m (<0.30) at sea surface were consequences of nitrogen deficiency and photo-inhibition. The well-developed SCM between 75 m and 100 m was consistent with the mixed layer depth and euphotic depth. Formation of SCM was a balance between nutrient availability and light limitation. Phytoplankton at sea surface presented lower light utilization efficiencies to exploit wider range of light intensity. Phytoplankton in the SCM presented higher light utilization efficiencies to guarantee higher photosynthetic efficiencies under light limited circumstances. The highest photosynthetic competence in the SCM highlighted the importance of SCM to the primary production and pelagic food web. These results provide insight into adaptation strategies of phytoplankton in the less studied eastern equatorial Indian Ocean.

Acknowledgements

We are grateful to the captain and crew of the R/V *Madidi-hang 03* for their assistance during the cruise. We thank Kaiming Sun for his assistance on the draft, Jingyu Zhang for her guidance on obtaining remote sensing data.

References

- Barlow R, Lamont T, Gibberd M J, et al. 2017. Phytoplankton communities and acclimation in a cyclonic eddy in the southwest Indian Ocean. *Deep Sea Research Part I: Oceanographic Research Papers*, 124: 18–30, doi: [10.1016/j.dsr.2017.03.013](https://doi.org/10.1016/j.dsr.2017.03.013)
- Bibby T S, Mary I, Nield J, et al. 2003. Low-light-adapted *Prochlorococcus* species possess specific antennae for each photosystem. *Nature*, 424(6952): 1051–1054, doi: [10.1038/nature01933](https://doi.org/10.1038/nature01933)
- Bouchard J N, Campbell D A, Roy S. 2005. Effects of UV-B radiation on the D1 protein repair cycle of natural phytoplankton communities from three latitudes (Canada, Brazil, and Argentina). *Journal of Phycology*, 41(2): 273–286, doi: [10.1111/\(ISSN\)1529-8817](https://doi.org/10.1111/(ISSN)1529-8817)
- Cullen J J. 2015. Subsurface chlorophyll maximum layers: Enduring enigma or mystery solved?. *Annual Review of Marine Science*, 7(1): 207–239, doi: [10.1146/annurev-marine-010213-135111](https://doi.org/10.1146/annurev-marine-010213-135111)
- Durako M J. 2012. Using PAM fluorometry for landscape-level assessment of *Thalassia testudinum*: Can diurnal variation in photochemical efficiency be used as an ecoindicator of seagrass health?. *Ecological Indicators*, 18: 243–251, doi: [10.1016/j.ecoind.2011.11.025](https://doi.org/10.1016/j.ecoind.2011.11.025)
- Edwards K F, Thomas M K, Klausmeier C A, et al. 2015. Light and growth in marine phytoplankton: allometric, taxonomic, and

- environmental variation. *Limnology and Oceanography*, 60(2): 540–552, doi: [10.1002/lno.10033](https://doi.org/10.1002/lno.10033)
- Eilers P H C, Peeters J H C. 1988. A model for the relationship between light intensity and the rate of photosynthesis in phytoplankton. *Ecological Modelling*, 42: 199–215, doi: [10.1016/0304-3800\(88\)90057-9](https://doi.org/10.1016/0304-3800(88)90057-9)
- Fernand L, Weston K, Morris T, et al. 2013. The contribution of the deep chlorophyll maximum to primary production in a seasonally stratified shelf sea, the North Sea. *Biogeochemistry*, 113(1–3): 153–166, doi: [10.1007/s10533-013-9831-7](https://doi.org/10.1007/s10533-013-9831-7)
- Field C B, Behrenfeld M J, Randerson J T, et al. 1998. Primary production of the biosphere: Integrating terrestrial and oceanic components. *Science*, 281(5374): 237–240, doi: [10.1126/science.281.5374.237](https://doi.org/10.1126/science.281.5374.237)
- George J V, Nuncio M, Chacko R, et al. 2013. Role of physical processes in chlorophyll distribution in the western tropical Indian Ocean. *Journal of Marine Systems*, 113–114: 1–12, doi: [10.1016/j.jmarsys.2012.12.001](https://doi.org/10.1016/j.jmarsys.2012.12.001)
- Halsey K H, Jones B M. 2015. Phytoplankton strategies for photosynthetic energy allocation. *Annual Review of Marine Science*, 7(1): 265–297, doi: [10.1146/annurev-marine-010814-015813](https://doi.org/10.1146/annurev-marine-010814-015813)
- Halsey K H, Milligan A J, Behrenfeld M J. 2014. Contrasting strategies of photosynthetic energy utilization drive lifestyle strategies in ecologically important picoeukaryotes. *Metabolites*, 4(2): 260–280, doi: [10.3390/metabo4020260](https://doi.org/10.3390/metabo4020260)
- Hanson C E, Pattiaratchi C B, Waite A M. 2005. Sporadic upwelling on a downwelling coast: Phytoplankton responses to spatially variable nutrient dynamics off the Gascoyne region of Western Australia. *Continental Shelf Research*, 25: 1561–1582, doi: [10.1016/j.csr.2005.04.003](https://doi.org/10.1016/j.csr.2005.04.003)
- Harrison J W, Silsbe G M, Smith R E H. 2015. Photophysiology and its response to visible and ultraviolet radiation in freshwater phytoplankton from contrasting light regimes. *Journal of Plankton Research*, 37(2): 472–488, doi: [10.1093/plankt/fbv003](https://doi.org/10.1093/plankt/fbv003)
- Hartig P, Wolfstein K, Lippemeier S, et al. 1998. Photosynthetic activity of natural microphytobenthos populations measured by fluorescence (PAM) and ¹⁴C-tracer methods: a comparison. *Marine Ecology Progress Series*, 166: 53–62, doi: [10.3354/meps166053](https://doi.org/10.3354/meps166053)
- Hong Lisha, Wang Chunsheng, Zhou Yadong, et al. 2012. The distribution of chlorophyll *a* in the tropical eastern Indian Ocean in austral summer. *Acta Oceanologica Sinica*, 31(5): 146–159, doi: [10.1007/s13131-012-0244-6](https://doi.org/10.1007/s13131-012-0244-6)
- Hopkinson B M, Mitchell B G, Reynolds R A, et al. 2007. Iron limitation across chlorophyll gradients in the southern Drake Passage: Phytoplankton responses to iron addition and photosynthetic indicators of iron stress. *Limnology and Oceanography*, 52(6): 2540–2554, doi: [10.4319/lo.2007.52.6.2540](https://doi.org/10.4319/lo.2007.52.6.2540)
- Idso S B, Gilbert R G. 1974. On the universality of the poole and atkins secchi disk-light extinction equation. *Journal of Applied Ecology*, 11(1): 399–401, doi: [10.2307/2402029](https://doi.org/10.2307/2402029)
- Ihnken S, Eggert A, Beardall J. 2010. Exposure times in rapid light curves affect photosynthetic parameters in algae. *Aquatic Botany*, 93(3): 185–194, doi: [10.1016/j.aquabot.2010.07.002](https://doi.org/10.1016/j.aquabot.2010.07.002)
- Kalaji H M, Carpentier R, Allakhverdiev S I, et al. 2012. Fluorescence parameters as early indicators of light stress in barley. *Journal of Photochemistry and Photobiology B: Biology*, 112: 1–6, doi: [10.1016/j.jphotobiol.2012.03.009](https://doi.org/10.1016/j.jphotobiol.2012.03.009)
- Kim Tiam S, Laviale M, Feurtet-Mazel A, et al. 2015. Herbicide toxicity on river biofilms assessed by pulse amplitude modulated (PAM) fluorometry. *Aquatic Toxicology*, 165: 160–171, doi: [10.1016/j.aquatox.2015.05.001](https://doi.org/10.1016/j.aquatox.2015.05.001)
- Lavaud J. 2007. Fast regulation of photosynthesis in diatoms: Mechanisms, evolution and ecophysiology. *Functional Plant Science and Biotechnology*, 1: 267–287
- Lavaud J, Strzpek R F, Kroth P G. 2007. Photoprotection capacity differs among diatoms: Possible consequences on the spatial distribution of diatoms related to fluctuations in the underwater light climate. *Limnology and Oceanography*, 52(3): 1188–1194, doi: [10.4319/lo.2007.52.3.1188](https://doi.org/10.4319/lo.2007.52.3.1188)
- Lee K, Matsuno T, Endoh T, et al. 2017. A role of vertical mixing on nutrient supply into the subsurface chlorophyll maximum in the shelf region of the East China Sea. *Continental Shelf Research*, 143: 139–150, doi: [10.1016/j.csr.2016.11.001](https://doi.org/10.1016/j.csr.2016.11.001)
- Li Gang, Lin Qiang, Ni Guangyan, et al. 2012. Vertical patterns of early summer chlorophyll *a* concentration in the Indian Ocean with special reference to the variation of deep chlorophyll maximum. *Journal of Marine Biology*, 2012: Article ID 801248
- Li Junlei, Sun Xiaoxia. 2014. Photosynthetic characteristics of phytoplankton in winter in the Jiaozhou Bay. *Oceanologia et Limnologia Sinica (in Chinese)*, 45: 468–479
- Li Junlei, Sun Xiaoxia, Zheng Shan. 2016. In situ study on photosynthetic characteristics of phytoplankton in the Yellow Sea and East China Sea in summer 2013. *Journal of Marine Systems*, 160: 94–106, doi: [10.1016/j.jmarsys.2016.03.016](https://doi.org/10.1016/j.jmarsys.2016.03.016)
- Lippemeier S, Hintze R, Vanselow K, et al. 2001. In-line recording of PAM fluorescence of phytoplankton cultures as a new tool for studying effects of fluctuating nutrient supply on photosynthesis. *European Journal of Phycology*, 36(1): 89–100, doi: [10.1080/09670260110001735238](https://doi.org/10.1080/09670260110001735238)
- Liu Huaxue, Ke Zhixin, Song Xingyu, et al. 2011. Primary production in the Bay of Bengal during spring intermonsoon period. *Acta Oceanologica Sinica (in Chinese)*, 31(23): 7007–7012
- Madhupratap M, Gauns M, Ramaiah N, et al. 2003. Biogeochemistry of the Bay of Bengal: physical, chemical and primary productivity characteristics of the central and western Bay of Bengal during summer monsoon 2001. *Deep Sea Research Part II: Topical Studies in Oceanography*, 50(5): 881–896, doi: [10.1016/S0967-0645\(02\)00611-2](https://doi.org/10.1016/S0967-0645(02)00611-2)
- Martin J, Tremblay J, Gagnon J, et al. 2010. Prevalence, structure and properties of subsurface chlorophyll maxima in Canadian Arctic waters. *Marine Ecology Progress Series*, 412: 69–84, doi: [10.3354/meps08666](https://doi.org/10.3354/meps08666)
- McMinn A, Hegseth E N. 2004. Quantum yield and photosynthetic parameters of marine microalgae from the southern Arctic Ocean, Svalbard. *Journal of the Marine Biological Association of the UK*, 84(5): 865–871, doi: [10.1017/S0025315404010112h](https://doi.org/10.1017/S0025315404010112h)
- Mino Y, Matsumura S, Lirdwitayaprasit T, et al. 2014. Variations in phytoplankton photo-physiology and productivity in a dynamic eutrophic ecosystem: a fast repetition rate fluorometer-based study. *Journal of Plankton Research*, 36(2): 398–411, doi: [10.1093/plankt/fbt118](https://doi.org/10.1093/plankt/fbt118)
- Moore C M, Seeyave S, Hickman A E, et al. 2007. Iron-light interactions during the CROZet natural iron bloom and EXport experiment (CROZEX) I: Phytoplankton growth and photophysiology. *Deep Sea Research Part II: Topical Studies in Oceanography*, 54(18–20): 2045–2065, doi: [10.1016/j.dsr2.2007.06.011](https://doi.org/10.1016/j.dsr2.2007.06.011)
- Moore C M, Suggett D J, Hickman A E, et al. 2006. Phytoplankton photoacclimation and photoadaptation in response to environmental gradients in a shelf sea. *Limnology and Oceanography*, 51(2): 936–949, doi: [10.4319/lo.2006.51.2.0936](https://doi.org/10.4319/lo.2006.51.2.0936)
- Parsons T R, Maita Y, Lalli C M. 1984. *A Manual of Chemical and Biological Methods for Seawater Analysis*. Toronto, Canada: Pergamon Press
- Ralph P J, Gademann R. 2005. Rapid light curves: a powerful tool to assess photosynthetic activity. *Aquatic Botany*, 82(3): 222–237, doi: [10.1016/j.aquabot.2005.02.006](https://doi.org/10.1016/j.aquabot.2005.02.006)
- Rao R R, Kumar M S G, Ravichandran M, et al. 2010. Interannual variability of Kelvin wave propagation in the wave guides of the equatorial Indian Ocean, the coastal Bay of Bengal and the southeastern Arabian Sea during 1993–2006. *Deep Sea Research Part I: Oceanographic Research Papers*, 57(1): 1–13, doi: [10.1016/j.dsr.2009.10.008](https://doi.org/10.1016/j.dsr.2009.10.008)
- Ryan K G, Cowie R O M, Liggins E, et al. 2009. The short-term effect of irradiance on the photosynthetic properties of Antarctic fast-ice microalgal communities. *Journal of Phycology*, 45(6): 1290–1298, doi: [10.1111/j.1529-8817.2009.00764.x](https://doi.org/10.1111/j.1529-8817.2009.00764.x)
- Sardessai S, Shetye S, Maya M V, et al. 2010. Nutrient characteristics of the water masses and their seasonal variability in the eastern equatorial Indian Ocean. *Marine Environmental Research*, 70(3–4): 272–282, doi: [10.1016/j.marenvres.2010.05.009](https://doi.org/10.1016/j.marenvres.2010.05.009)
- Schott F A, McCreary J P Jr. 2001. The monsoon circulation of the In-

- dian Ocean. *Progress in Oceanography*, 51(1): 1–123, doi: [10.1016/S0079-6611\(01\)00083-0](https://doi.org/10.1016/S0079-6611(01)00083-0)
- Schreiber U. 2004. Pulse-Amplitude-Modulation (PAM) fluorometry and saturation pulse method: An overview. In: Papageorgiou G C, Govindjee, eds. *Chlorophyll a Fluorescence. Advances in Photosynthesis and Respiration*, vol 19. Netherlands: Springer, 279–319
- Schreiber U, Bilger W, Neubauer C. 1995. Chlorophyll fluorescence as a noninvasive indicator for rapid assessment of in vivo photosynthesis. In: Schulze E D, Caldwell M M, eds. *Ecophysiology of Photosynthesis*. Berlin, Heidelberg: Springer, 49–70
- Sharon Y, Beer S. 2008. Diurnal movements of chloroplasts in *Halophila stipulacea* and their effect on PAM fluorometric measurements of photosynthetic rates. *Aquatic Botany*, 88(4): 273–276, doi: [10.1016/j.aquabot.2007.11.006](https://doi.org/10.1016/j.aquabot.2007.11.006)
- Sharples J, Moore M C, Rippeth T P, et al. 2001. Phytoplankton distribution and survival in the thermocline. *Limnology and Oceanography*, 46(3): 486–496, doi: [10.4319/lo.2001.46.3.0486](https://doi.org/10.4319/lo.2001.46.3.0486)
- Six C, Finkel Z V, Rodriguez F, et al. 2008. Contrasting photoacclimation costs in ecotypes of the marine eukaryotic picoplankter *Ostreococcus*. *Limnology and Oceanography*, 53(1): 255–265, doi: [10.4319/lo.2008.53.1.0255](https://doi.org/10.4319/lo.2008.53.1.0255)
- Strutton P G, Coles V J, Hood R R, et al. 2014. Biogeochemical variability in the equatorial Indian Ocean during the monsoon transition. *Biogeosciences Discussions*, 11: 6185–6219, doi: [10.5194/bgd-11-6185-2014](https://doi.org/10.5194/bgd-11-6185-2014)
- Suggett D J, Prášil O, Borowitzka M A. 2010. *Chlorophyll a Fluorescence in Aquatic Sciences: Methods and Applications*. Dordrecht, Netherlands: Springer
- Thompson P A, Pesant S, Waite A M. 2007. Contrasting the vertical differences in the phytoplankton biology of a dipole pair of eddies in the south-eastern Indian Ocean. *Deep Sea Research Part II: Topical Studies in Oceanography*, 54(8-10): 1003–1028, doi: [10.1016/j.dsr2.2006.12.009](https://doi.org/10.1016/j.dsr2.2006.12.009)
- Wagner H, Jakob T, Wilhelm C. 2006. Balancing the energy flow from captured light to biomass under fluctuating light conditions. *New Phytologist*, 169(1): 95–108, doi: [10.1111/nph.2006.169.issue-1](https://doi.org/10.1111/nph.2006.169.issue-1)
- Wang Xiaodong, Jiang Tao, Cen Jingyi, et al. 2012. Photosynthetic characteristics of phytoplankton in the Daya Bay. *Oceanologia et Limnologia Sinica (in Chinese)*, 43: 589–594
- White S, Anandraj A, Bux F. 2011. PAM fluorometry as a tool to assess microalgal nutrient stress and monitor cellular neutral lipids. *Bioresource Technology*, 102(2): 1675–1682, doi: [10.1016/j.biortech.2010.09.097](https://doi.org/10.1016/j.biortech.2010.09.097)
- Wiggert J D, Murtugudde R G, Christian J R. 2006. Annual ecosystem variability in the tropical Indian Ocean: Results of a coupled bio-physical ocean general circulation model. *Deep Sea Research Part II: Topical Studies in Oceanography*, 53(5-7): 644–676, doi: [10.1016/j.dsr2.2006.01.027](https://doi.org/10.1016/j.dsr2.2006.01.027)
- Wyrtki K. 1973. An equatorial jet in the Indian Ocean. *Science*, 181(4096): 262–264, doi: [10.1126/science.181.4096.262](https://doi.org/10.1126/science.181.4096.262)
- Xue Bing, Sun Jun, Ding Changling, et al. 2016. Diatom communities in equatorial region and its adjacent areas of eastern Indian Ocean during spring intermonsoon 2014. *Haiyang Xuebao (in Chinese)*, 38(2): 112–120
- Zhang Min, Kong Fanxiang, Wu Xiaodong, et al. 2008. Different photochemical responses of phytoplankters from the large shallow Taihu Lake of subtropical China in relation to light and mixing. *Hydrobiologia*, 603(1): 267–278, doi: [10.1007/s10750-008-9277-4](https://doi.org/10.1007/s10750-008-9277-4)
- Zhang Wenquan, Wang Baodong, Wei Qinsheng, et al. 2016. Spatial distribution of primary nitrite maximum and its influencing factors in the east Indian Ocean in spring. *Advances in Marine Science (in Chinese)*, 34(3): 403–410
- Zhou Yadong, Wang Chunsheng, Wang Xiaogu, et al. 2011. The distribution of size-fractionated chlorophyll a in the Indian Ocean South Equatorial Current. *Acta Ecologica Sinica (in Chinese)*, 31(16): 4586–4598